Systematic arcminute-scale fixational offsets in patients with early visual cortex damage

Ashley M. Clark * Department of Brain & Cognitive Sciences and Center for Visual Science, University of Rochester, Rochester, NY, USA

Sanjana Kapisthalam * Department of Brain & Cognitive Sciences and Center for Visual Science, University of Rochester, Rochester, NY, USA

Matthew R. Cavanaugh Department of Ophthalmology, Flaum Eye Institute and Center for Visual Science, University of Rochester, Rochester, NY, USA

Krystel R. Huxlin † Department of Ophthalmology, Flaum Eye Institute and Center for Visual Science, University of Rochester, Rochester, NY, USA

Martina Poletti † Department of Brain & Cognitive Sciences and Center for Visual Science, University of Rochester, Rochester, NY, USA

Cortically induced blindness (CB) resulting from stroke damage to the early visual cortex leads to extensive, typically extrafoveal visual deficits and is known to alter large-scale oculomotor behavior. Here, we show that even with preserved foveal acuity, fixational oculomotor behavior is subtly altered in CB patients. Using high-precision eye tracking, we observed a small but consistent gaze offset toward the blind field during passive fixation, which disappeared during a high-acuity central task. Despite this offset, fixation precision in both tasks was comparable, and it was similar between CB patients and age-matched controls. Curiously, the underlying oculomotor dynamics were also similar across the two task conditions: Microsaccades exhibited nonsignificant directional tendencies, while ocular drift was biased away from the blind field. Our findings indicate that the adult oculomotor system dynamically adapts to asymmetric visual injury and/or input. We speculate that the small fixational offsets observed in CB may reflect an attentional pointer toward the blind field and/or a compensatory oculomotor rebalancing that counteracts an asymmetric visual drive following cortical damage. Together, these results reveal a surprising preservation of context-dependent fixation control following early visual cortex damage in adulthood.

Introduction

Worldwide, between 20% and 57% of strokes result in vision loss, often referred to as cortically induced blindness or CB (Pollock et al., 2019; Rowe & VIS Writing Group, 2017; Sand et al., 2013). This type of blindness is caused by damage to early visual cortical areas in the occipital lobe of the brain and may ultimately affect nearly 1% of adults older than 49 years (Gilhotra, Mitchell, Healey, Cumming, & Currie, 2002). In CB, the stroke is often unilateral, and the impact on the visual field is homonymous (i.e., affecting the same parts of the field through both eyes). The extent and severity of vision loss in CB vary based on the amount and location of damage to the early visual cortex. Furthermore, the characteristics of the blind field can differ greatly in terms of size and proximity to central vision, although the foveal representation is often spared (Horton, Economides, & Adams, 2021). Although individuals with CB range widely in their ability to perform basic visually guided actions, among other impairments, they often report challenges that negatively affect their social-emotional health (Bauer et al., 2023; Dogra et al., 2024).

Citation: Clark, A. M., Kapisthalam, S., Cavanaugh, M. R., Huxlin, K. R., & Poletti, M. (2026). Systematic arcminute-scale fixational offsets in patients with early visual cortex damage. *Journal of Vision*, *26*(2):5, 1–15, https://doi.org/10.1167/jov.26.2.5.

https://doi.org/10.1167/jov.26.2.5 Received June 30, 2025; published February 10, 2026 ISSN 1534-7362

In contrast with other common vision disorders of retinal origin, in CB, there is considerable residual information processing in the blind field, a phenomenon first described by Riddoch (1917) and later studied in the context of "blindsight" (Weiskrantz, 1996; Weiskrantz, 2009; Weiskrantz, Warrington, Sanders, & Marshall, 1974). Yet, in the case of a unilateral stroke, unconscious visual processing in the blind field is of little practical benefit in everyday life; partly as a result of this, individuals with CB are instead encouraged to use substitution (Bowers, Keeney, & Peli, 2008) or adopt compensatory strategies to capture the visual information needed for specific tasks (Bowers et al., 2008; Jung & Peli, 2018; Pollock et al., 2019; Roth et al., 2009; Trauzettel-Klosinski & Reinhard, 1998; Zihl, Kentridge, Pargent, & Heywood, 2021). In the former case, patients are trained to use prisms that shift peripheral visual information to spared portions of the central field. In the latter case, patients are trained to strategically shift gaze to capture the information needed. An alternative strategy, however, is to use perceptual training protocols to restore visual discrimination abilities in affected portions of the visual field, often in combination with attentional strategies, which leverage top-down mechanisms to enhance usage and processing of information from impaired regions of the visual field (Cavanaugh, Barbot, Carrasco, & Huxlin, 2019; Cavanaugh, Carrasco, & Huxlin, 2025; Cavanaugh, Tadin, Carrasco, & Huxlin, 2022). In everyday life, information such as oncoming traffic may not be perceived unless the visuomotor system actively attends to relevant stimuli and shifts gaze strategically to compensate for the vision loss (Giudice, 2018). Interestingly, even without training, CB patients saccade more frequently toward their blind field (Iorizzo, Riley, Hayhoe, & Huxlin, 2011; Kerkhoff, 1999) and may exhibit shorter fixation durations (Pambakian et al., 2000). This happens despite (or, perhaps, because of) deficient preprocessing of peripheral information prior to making saccades into their blind field (Kwon, Fahrenthold, Cavanaugh, Huxlin, & Mitchell, 2022). Nonetheless, by moving their eyes toward the blind field, individuals effectively position visual information from their blind periphery into their (usually unaffected) foveal and parafoveal fields.

Although changes in oculomotor behavior have been reported for visually guided activities such as reading (Trauzettel-Klosinski, 1997; Trauzettel-Klosinski & Reinhard, 1998), scanning the world (Pambakian et al., 2000), detecting stimuli (Gao & Sabel, 2017), or attempting to detect moving objects in a naturalistic virtual environment (Iorizzo et al., 2011), we do not know if and how unilateral CB systematically alters aspects of fine-scale eye movements, such as ocular drift and microsaccades, during sustained fixation and when performing tasks requiring visual acuity. Small eye movements continually shift the retinal projection of objects during fixation (Ahissar & Arieli, 2012; Barlow, 1952; Ratnam, Domdei, Harmening, & Roorda, 2017; Rucci & Poletti, 2015; Rucci & Victor, 2015). Drift exhibits a Brownian motion profile and is constantly present during the time period when visual information is acquired. Microsaccades, on the other hand, resemble larger saccades, but with smaller amplitudes and velocity; they reorient gaze on a much smaller scale to allow for visual exploration of fine detail in the center of gaze inside the fovea (Cherici, Kuang, Poletti, & Rucci, 2012; Poletti, Listorti, & Rucci, 2013; Shelchkova, Tang, & Poletti, 2019). These eye movements have been shown to play an important role in fine spatial vision and visual acuity (Anderson, Ratnam, Roorda, & Olshausen, 2020; Clark, Intoy, Rucci, & Poletti, 2022; Intoy & Rucci, 2020; Poletti et al., 2013; Steinman, Haddad, Skavenski, & Wyman, 1973; Witten, Lukyanova, & Harmening, 2024). Even if, in most cases of CB, central vision is preserved, here we show that CB affects fixational eye movements without impairing fixational precision. Our findings highlight an interdependence of peripheral and foveal processing and the fact that missing, reduced, or abnormal visual processing in the peripheral field of view caused by early visual cortex damage may bias the centering of gaze during fixation and alter the balance between microsaccade and drift directions.

Methods

Participants

We recruited 15 adult CB patients (10 men and 5 women) with an average age of 54 ± 15 years (Table 1), who were between ∼1.3 and 130 months post-unilateral occipital stroke. Participants had homonymous visual field defects but exhibited no ocular or cognitive deficits, including neglect. The extent and location of the damage in the occipital cortex were verified through inspection of structural brain images, which included magnetic resonance imaging (MRI) or computed tomography scans. In addition to the patient group, 13 healthy, naive age-matched control subjects and 1 experienced observer, who is also an author, participated in the study, resulting in a total of 14 control subjects (2 men and 12 women) with an average age of 43 ± 11 years.

This study was approved by the University of Rochester's Research Subjects Review Board, and all procedures complied with the tenets of the Declaration of Helsinki. Prior to participating, all subjects received a detailed explanation of the experiment and reviewed the materials included in the consent form. After demonstrating understanding of the information

Subject ID	Sex	Years of age	Snellen acuity (20/X)	Weeks poststroke
CB1	F	29	16.96	186.1
CB2	F	42	21.22	5.0
CB3	M	43	23.91	11.9
CB4	M	55	24.92	249.6
CB5	M	61	23.80	14.4
CB6	M	75	61.80	123.9
CB7	M	48	18.22	35.0
CB8	M	68	40.74	27.6
CB9	M	60	29.33	520.4
CB10	M	68	46.71	10.3
CB11	F	40	41.22	26.6
CB12	F	49	22.57	24.0
CB13	M	68	96.40	159.7
CB14	M	72	29.28	53.1
CB15	F	28	19.06	14.6
S1	F	50	23.71	—
S2	M	46	45.74	—
S3	F	25	16.84	—
S4	F	40	27.87	—
S5	F	42	26.42	—
S6	F	28	15.69	—
S7	M	59	23.67	—
S8	F	59	34.85	—
S9	F	41	24.93	—
S10	F	50	21.60	—
S11	F	52	20.00	—
S12	F	43	14.20	—
S13	F	35	20.00	—
S14	F	31	41.90	—

Table 1. Participant demographics. Stroke participants are labeled with CB identifiers; visually intact controls are denoted as S1–S14. *Note:* F = female; M = male. Snellen acuity scores are reported with letter-level precision by adjusting the denominator to reflect the number of letters missed per line.

and providing verbal consent to participate, written informed consent was obtained and documented.

Subjects were tested using a Tumbling E acuity test with a digital duo-chrome red/green background to determine refractive error and screen for eligibility. Individuals with uncorrected acuity worse than 20/100 were excluded from enrollment. To correct for spherical error, a custom-made Badal optometer was used. This system allowed for +3 D to −8 D spherical error to be corrected for each subject, while keeping the image size in visual angle the same across all corrections (Atchison, Bradley, Thibos, & Smith, 1995). All subjects used a Badal optometer to self-correct as necessary, with a minimum requirement of achieving 20/50 Snellen acuity. All subjects viewed stimuli in both the fixation and acuity tasks through the optometer.

To define the location, severity, and boundaries of their visual field defects, CB participants underwent monocular 10-2 and 24-2 Humphrey visual field (HVF) tests of the right eye using a Humphrey Field Analyzer II-i 750. Testing patterns were probed with white, Goldmann size III stimuli (Zeiss Humphrey Systems, Dublin, CA, USA). The 24-2 pattern included 54 locations with a sampling interval of 6 degrees, covering the central 42 degrees of the visual field. The 10-2 pattern tested 68 locations with a sampling interval of 2 degrees, covering the central 18 degrees of the visual field. Tests were performed with controlled fixation, using the Gaze/Blind Spot automatic settings, visual acuity corrected to 20/20, and a background luminance of 11.3 cd/m^2. Standardized STATPAC software (Humphrey STATPAC; Zeiss Humphrey Systems) was used to estimate performance.

Psychophysics apparatus (Figure 1A)

Stimuli were delivered monocularly to participants' right eyes, with the left eye covered. Data were collected in one to two experimental sessions. Each session lasted approximately 3 hours, and most participants (23/29) completed data collection within one session.

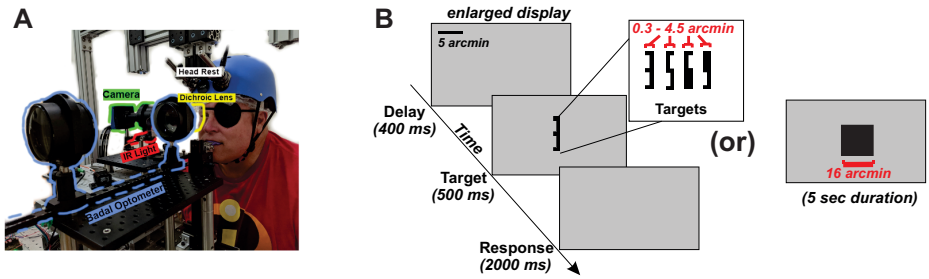

Figure 1. **Experimental setup and psychophysical paradigm.** (**A**) Eye movements were recorded using a custom-built digital dual-Purkinje image eye tracker. During tracking, participants were best corrected for vision using a Badal optometer (highlighted in blue). (**B**) Participants completed two tasks on interleaved trials, presented monocularly: a fixation task and a high-acuity number identification task. Each trial began with a brief blank screen to eliminate any image aftereffects, followed by presentation of either a fixation target or high-acuity stimuli in Pelli font. Participants identified the number stimuli using a handheld controller. After every two acuity task trials, they performed a fixation trial, during which they were required to fixate on a central 16′ × 16′ square marker for 5 s.

Every session started with preliminary setup operations that lasted a few minutes, first involving comfortably positioning the observer to be stationary in the eye-tracking apparatus. This was achieved by using a combination of a custom-made bite bar as well as a helmet that attached to the system with magnets. Eye position was recorded using a custom-built dDPI eye tracker (Wu et al., 2023) (Figure 1A) operating at 340 Hz, coupled with a system for gaze-contingent display control (Santini, Redner, Iovin, & Rucci, 2007), enabling more accurate localization of the line of sight than commercial eye trackers (Poletti & Rucci, 2016). This system achieves a spatial resolution of at least 1 arcmin and exhibits internal noise well below 1 arcmin (Ko, Snodderly, & Poletti, 2016; Wu et al., 2023). Once the participant was comfortably positioned in the eye-tracking apparatus, the next steps included tuning the eye tracker for optimal performance and executing a two-step, gaze-contingent calibration procedure to map the eye tracker's output into visual angle. To ensure higher precision in eye tracking, participants viewed stimuli without glasses or contact lenses, and their vision was corrected using a spherical lens and a Badal optometer (Atchison et al., 1995).

Stimuli were shown on an LCD monitor (ASUS PG258Q; ASUS, China), with a vertical refresh rate of 200 Hz and a spatial resolution of 1,920 × 1,080 pixels. The monitor was 5 m away from the observer, and the observable screen distance changed based on the Badal optometer correction (varying from 3,900 to 5,100 mm; pixel-to-arcmin resolution varied from 0.25′ to 0.19′ per pixel).

Calibration procedure

In the first phase of the calibration procedure, an automatic calibration phase, observers sequentially fixated on each of the nine points of a 3 × 3 grid. The grid points were spaced 1.25 degrees apart horizontally and 50 arcmin vertically. In the second phase, referred to as manual calibration, observers confirmed or adjusted the mapping provided by the automatic calibration. Observers fixated on each of the nine grid points again, while the estimated location of the line of sight (based on the automatic calibration) was displayed in real time on the screen. Observers used a joypad to make fine adjustments to the predicted gaze location if necessary. Before each trial, the manual calibration procedure was repeated for the central position to account for any microscopic head movements and system drift that could occur, even with the use of a bite bar. This procedure ensured that the eye tracker's estimation of gaze aligned with the participant's perception of where their gaze should be on the monitor. This double-step calibration procedure improves line-of-sight localization by approximately one order of magnitude compared to standard methods (Poletti & Rucci, 2016).

Fixation and acuity tasks (Figure 1B)

In *fixation task trials*, subjects were asked to maintain fixation on a 16′ × 16′ marker at the center of the display for 5 s. Fixation task trials were presented once every two acuity task trials.

In *acuity task trials*, a target was presented at the center of the display. The target consisted of one of four possible digits (3, 5, 6, and 9) in Pelli font (Pelli et al., 2016). Stimuli were shown in black on a mid-gray background (RGB value 127, corresponding to 50% of the full 0–255 range), with a mean luminance of 18 cd/m^2. Each trial began with a blank fixation interval to eliminate afterimages of the preceding fixation marker. The central area where to maintain fixation was highlighted by peripheral arches. The blank interval

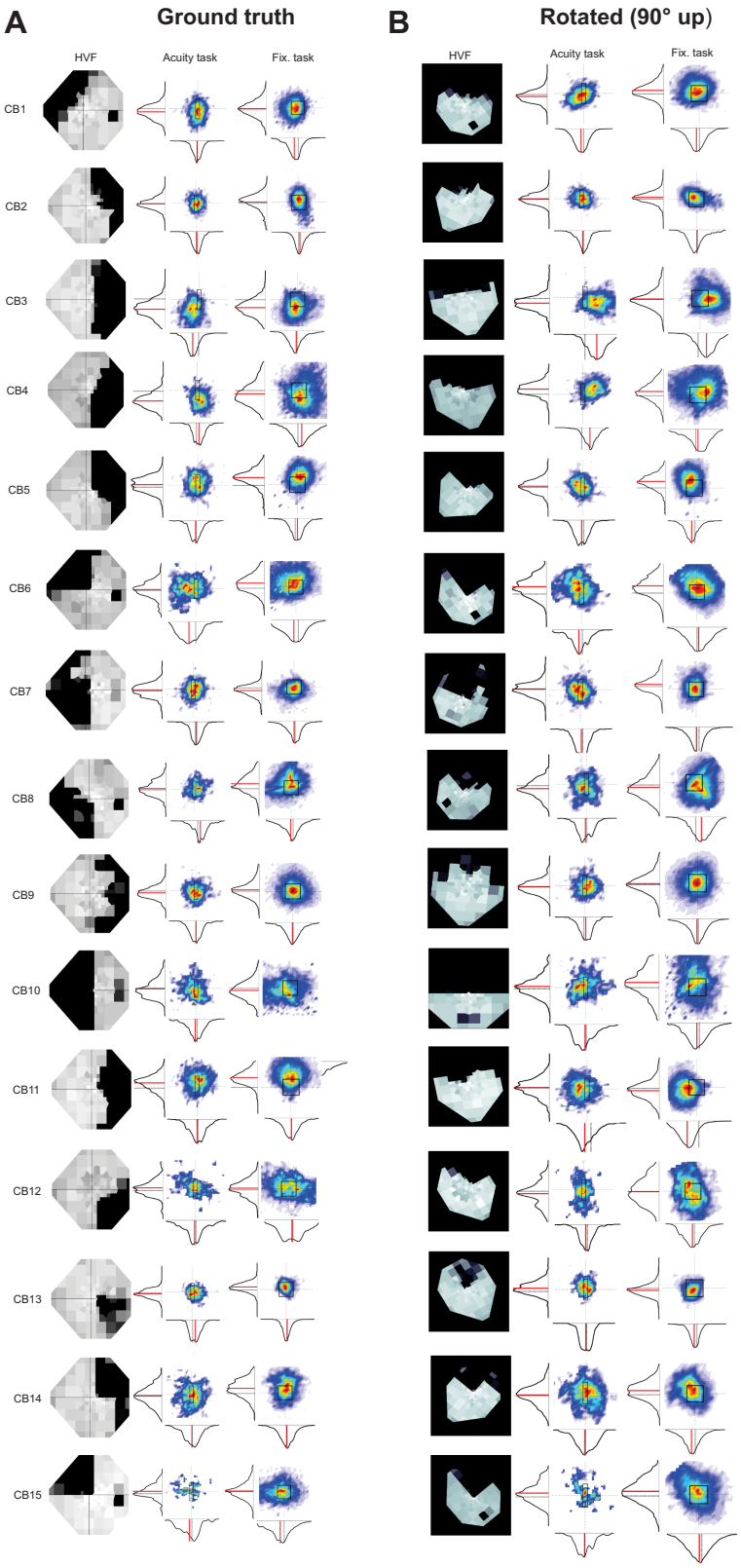

Figure 2. **Individual patients' ground truth and rotated HVFs, with corresponding two-dimensional gaze maps.** Each row represents a patient (CB1 to CB15). (**A**) Column 1: ground-truth HVF maps with panels displaying a grayscale map of visual sensitivity in decibels (dB), with darker shades indicating lower sensitivity (closer to 0 dB) and lighter shades denoting higher sensitivity (up to 50 dB). Visual fields cover the central 27 degrees (horizontal) × 21 degrees (vertical) by combining data from the Humphrey 24-2 and 10-2 test grids. Column 2: two-dimensional gaze distribution during the acuity task. Column 3: two-dimensional gaze distribution during the fixation task. (**B**) Corresponding, rotated versions of each map from A, with center of mass of the deficit at 90 degrees north.

was then followed by the target presentation. After the stimulus disappeared, participants reported the identity of the target digit using a handheld controller (Figure 1B). Stimulus size was adjusted using the parametric estimation by sequential testing procedure, based on subject performance. Stimulus sizes ranged from 0.38 to 82.08 arcmin in width.

Data analysis

Estimating the center of mass of visual field defects (Supplementary Figure S1)

Visual field defects were only analyzed for individuals with diagnosed visual field loss. First, the 10-2 and 24-2 HVF test results were combined into a single map to evaluate individuals' sensitivity over a wide field of view (24 degrees) but with increased resolution within the central ±10 degrees (Supplementary Figure S1). This combined map was then used to compute the overall sensitivity (in dB) across radial directions extending from the center of gaze (0 to 360 degrees, in 15-degree increments). Sensitivity in each direction was computed as the sum of the sensitivities of test points lying along the defined angle. For subjects with a blind field, a threshold sensitivity was defined as the average sensitivity across all tested locations in the visual field, including those toward the blind field. Radial directions were classified as showing a deficit if their sensitivity fell below this threshold. The average of all deficit directions was then computed and defined as the center of mass of the visual field loss for each patient.

Eye movements

Eye movements were categorized into two main groups: saccades (including microsaccades) and ocular drift. Eye movements with a minimal amplitude of 3 arcmin and a peak velocity higher than 3 degrees/s were selected as saccadic events. Saccades with amplitudes less than 30 arcmin were defined as microsaccades. Ocular motion between saccades was defined as drift. Classification of these eye movements was first performed automatically, then reviewed by an expert experimenter. Trials containing saccades, blinks, and/or bad tracking during stimulus presentation were removed. Furthermore, trials in which subjects did not respond or in which gaze deviated by more than ±3 degrees from the central fixation point at the beginning of the trial were excluded (on average, 5.2% of total trials; 4% due to initial gaze deviation, 1.2% due to no response).

Drift and microsaccade direction

Because the affected visual field location varied across CB patients, all HVFs were rotated such that the center of mass of the deficit was positioned vertically upward (90 degrees), and eye movement traces were rotated accordingly. This allowed us to use a common reference frame across patients. Eye movement directions were then classified as toward (0–180 degrees) or away (180–360 degrees) from the blind field. Since drift often changes direction, to determine the overall direction of each drift segment, we computed the average instantaneous direction, whereas microsaccade direction was computed based on the starting and landing positions. Figure 2A displays the individual, original HVFs for all patients along with their corresponding, rotated maps (Figure 2B). Supplementary Figure S2 displays individual gaze maps for all healthy controls.

Estimation of acuity thresholds

Visual acuity threshold (i.e., the minimum target stimulus width on acuity task trials required to perform reliably above chance level; 62.5% correct, with a 25% chance level) was determined using a cumulative Gaussian psychometric function fitted to the raw performance data (Wichmann & Hill, 2001). Better acuity corresponded to lower width threshold values.

Data and code availability

All data and MATLAB scripts used to create the figures in the article have been uploaded to the Open Science Framework repository. MATLAB was used to perform all statistical analyses.

Results

Fixational behavior during the sustained fixation task

To assess fixation precision when participants were asked to maintain fixation on a 16-arcmin × 16-arcmin marker presented at the center of the screen for 5 s, we computed a fixation, the bivariate contour ellipse area (BCEA), encompassing ± 1 *SD* of the two-dimensional distribution of gaze position. The BCEA measured, on average, 0.17 ± 0.05 deg^2 for patients and 0.14 ± 0.03 deg^2 for controls. A two-tailed unpaired *t*-test showed no significant difference between the two ($t_{27} = 1.24$, $p = 0.22$, Cohen's $d = 0.44$; Figure 3A), suggesting that fixation precision was comparable in CB patients and controls in this task. Furthermore, the variance did not differ significantly between patients and controls (*F*-test, $p = 0.20$).

We then analyzed how the Euclidean distance of the average gaze position from the center of the fixation

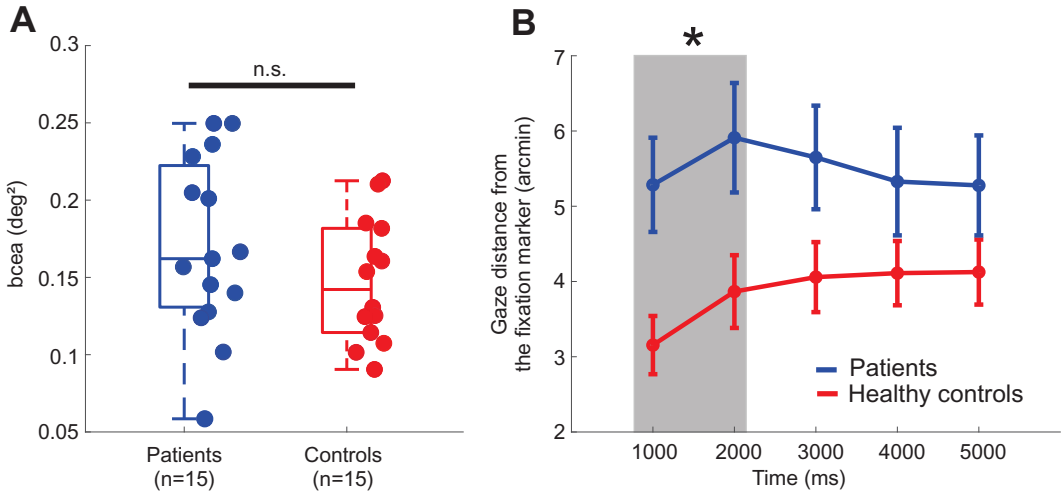

Figure 3. **Fixation stability during fixation trials.** (**A**) BCEA (area encompassing 68% of fixation points) in patients and controls. Box boundaries represent the 25th and 75th percentiles, and individual data points reflect single-subject measurements. There was no significant (n.s.) difference between the two groups (see main text for statistics). (**B**) Euclidean distance of the average gaze position during each 1-s interval from the center of the fixation marker (0,0) across the 5-s duration of fixation trials. Patients exhibited greater gaze deviation (5.28′ ± 2.4′) than controls (3.15′ ± 1.4′) during the first 2 s. The shaded region and asterisk indicate a statistically significant group difference. Error bars are *SEM*.

marker changed over time during fixation. CB patients exhibited a significantly greater gaze offset from the fixation center during the first 2 s compared to controls (Figure 3B; 0–2,000 ms: patients = 5.28′ ± 2.4′, controls = 3.15′ ± 1.4′; two-tailed unpaired *t*-test, $t_{27} = 2.84$, $p = 0.008$, Cohen's $d = 1.02$). These findings demonstrate that the difference between groups emerged immediately after fixation onset, with patients already exhibiting greater offset within the initial 2-s period.

To determine if patients' gaze position was affected by their blind field, we computed the center of mass (COM) angle of the unrotated fixation distributions for each subject and compared it to the COM angle of their individual lesions. We found that the subject's fixation COM fell within ± 90 degrees from the lesion COM, with an average difference of 47.19 ± 37.43 degrees (Figure 4).

We further examined their gaze position with respect to the COM of the blind field, aligned at 90 degrees on the vertical axis for every patient (see Methods for details). CB patients displayed a small "vertical" (y-axis) gaze offset (patients vs. controls: 2.3′ ± 3.1 vs. −1′ ± 3; two-tailed unpaired *t*-test: $t_{27} = 2.9$, $p = 0.006$, Cohen's $d = 1.05$; Figure 5A). For patients, this gaze offset was toward the COM of their blind field. Importantly, with respect to the x-axis, which had no directional correlation with the blind field when aligned at 90 degrees on the vertical axis, we observed no significant differences in (horizontal) offset between patients (–1.1′ ± 4.4′) and controls (0.55′ ± 2.4′; two-tailed unpaired *t*-test: $t_{27} = -1.2$, $p = 0.22$, Cohen's $d = -0.44$). In sum, patients' gaze was systematically offset *toward* the part of the visual field affected by vision loss during the fixation task (Figure 5B). Notably, neither patients (Figure 2A) nor controls (Figure 5C, Supplementary Figure S2) displayed systematic directional offsets when their average gaze maps were plotted in true space.

Next, we asked if the observed fixational bias toward the blind field in CB patients was a spurious effect of eye movement patterns or noise by conducting a simulation-based control analysis. We randomly rotated each patient's fixation data 1,000 times and computed the resulting mean fixation positions. If the original bias was due to random variability, the distribution of mean positions from these rotations would resemble the observed data in Figure 5A. However, the simulated data (Supplementary Figure S3) did not reproduce the systematic bias seen in the original (blind field–aligned) fixations (patients: 0.03′ ± 0.17′; controls: −1.04′ ± 2.9′; two-tailed unpaired *t*-test: $t_{27} = 1.4$, $p = 0.17$, Cohen's $d = 0.5$), indicating that the patients' bias is in fact direction-specific and not a general artifact of fixational behavior. Therefore, although the overall precision of fixation was similar in patients and controls, gaze distance from the fixation marker was larger in patients, who were characterized by a small but significant gaze offset in the direction of the blind field.

Finally, we examined the oculomotor behavior underlying the small gaze offsets toward the blind field during the fixation task. Eye movements were separated into microsaccades (5′–30′ in amplitude) and ocular drift. Microsaccade rate was comparable between CB patients and controls (patients: 1.4 ± 0.74 microsaccades/s; controls: 1.7 ± 0.73 microsaccades/s; two-tailed unpaired *t*-test: $t_{27} = -1.17$, $p = 0.24$, Cohen's $d = -0.42$), and there was no significant difference in

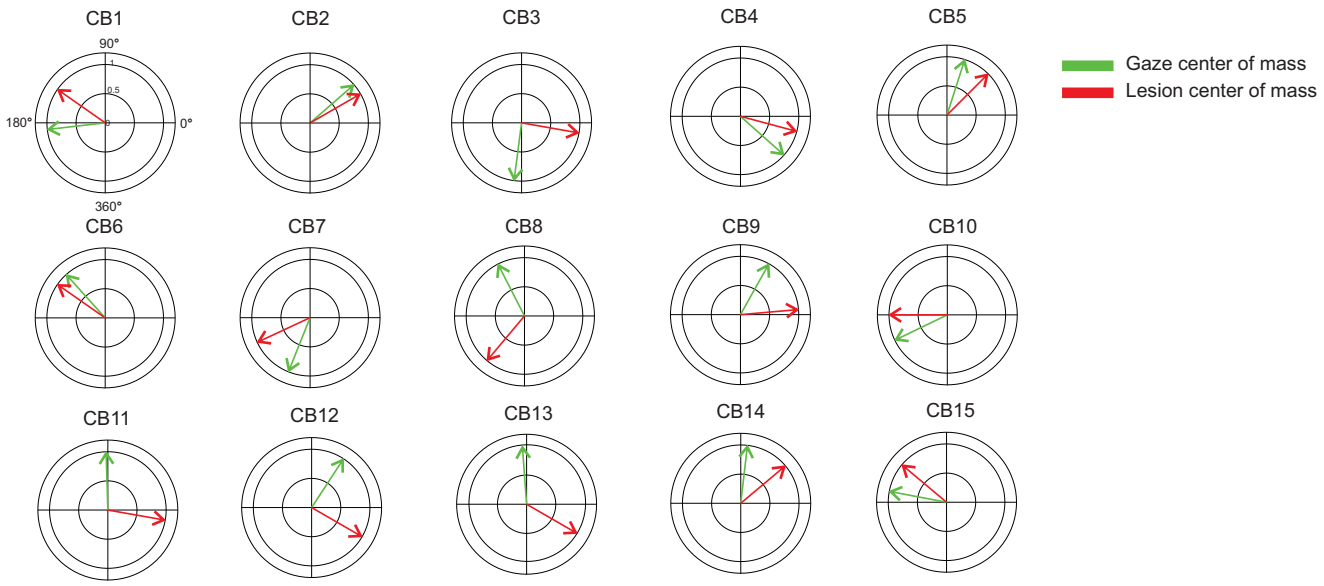

Figure 4. **Center of mass (COM) of fixation vs. lesion location.** For each subject, the COM angle of the unrotated fixation distribution (green arrow) and the COM angle of the individual lesion (red arrow). Fixation COMs fell within ±90 degrees of the lesion COM for most patients, with an average angular difference of 47.19 ± 37.43 degrees.

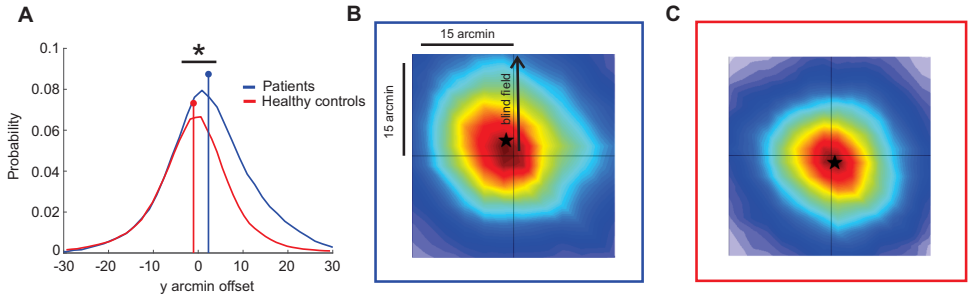

Figure 5. **Gaze distribution in fixation trials.** (**A**) Average gaze position distribution along the vertical (y) axis during fixation. For patients, individual gaze distributions (and corresponding visual deficits) were rotated such that the center of mass of the blind-field deficit was positioned at 90 degrees (vertical). For controls, gaze data are shown in their native coordinate frame (i.e., without rotation). Patients exhibited a small but statistically significant shift (toward the blind field). (**B**) Two-dimensional average gaze distribution across all patients, with gaze maps rotated such that the center of mass of the blind-field deficit faced upward (90 degrees). Note that the offset of CB patients' gaze distributions does not mean that subjects demonstrated an upward shift in gaze toward true north; rather, gaze was shifted toward each individual's respective blind field. (**C**) Corresponding average gaze distribution in healthy controls during fixation, shown in true (unrotated) visual space. Black stars (**B, C**) indicate the average gaze offset from the center fixation (0, 0).

the overall veridical direction of microsaccades across groups (Figure 6A; 0–180 degrees [upward] vs. 180–360 degrees [downward], unpaired t-test: $t_{26} = -1.79$, $p = 0.08$, Cohen's $d = -0.6$). However, microsaccades directed toward the blind field during the first 500 ms of the fixation task were slightly larger than those directed away (Figure 7; toward – away: 2.7 ± 3.4 arcmin, $p = 0.01$, paired t-test). Ocular drift characteristics, on the other hand, did not differ significantly between patients and controls (Figure 6D; 0–180 degrees vs. 180–360 degrees, unpaired t-test: $t_{27} = -1.90$, $p = 0.06$, Cohen's $d = -0.6$).

However, when the direction of these eye movements was analyzed relative to each patient's blind field—specifically, the center of mass of the scotoma—a distinct pattern emerged. Whereas microsaccades were equally likely to be directed toward or away from the blind field (Figures 6B, 6C; 50% ± 11% vs. 49% ± 11%; two-tailed paired t-test: $t_{13} = 0.31$, $p = 0.75$), ocular drift showed a directional bias away from the blind field (Figures 6E, 6F; toward vs. away from blind field: 12% ± 5% vs. 17% ± 5%; two-tailed paired t-test: $t_{14} = -2.35$, $p = 0.03$). In sum, although microsaccade direction remained balanced in CB patients and their

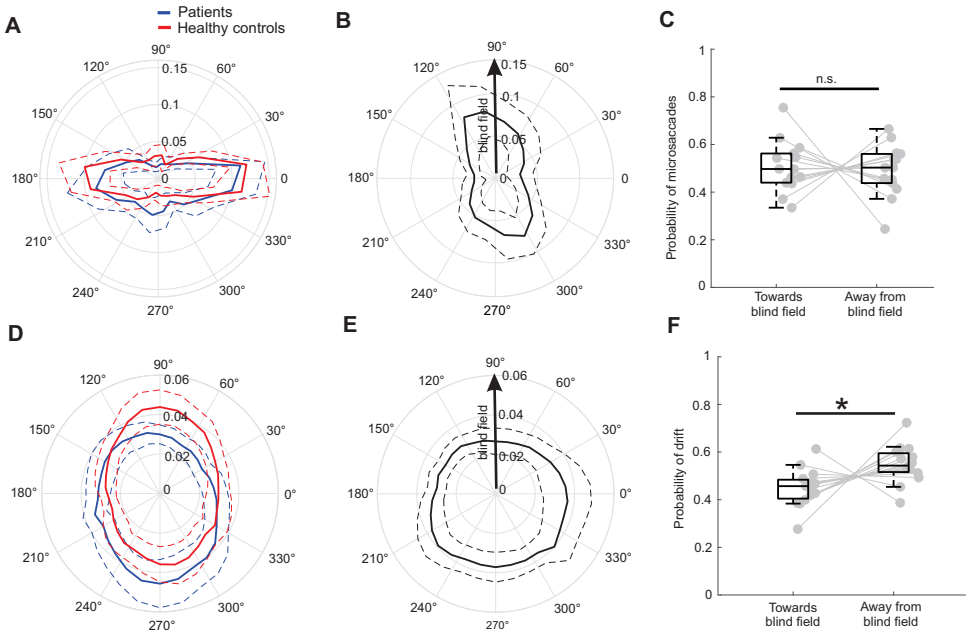

Figure 6. **Microsaccade and drift characteristics during the fixation task.** (**A**) Average microsaccade direction of CB patients (blue) and controls (red), plotted with respect to angle in real space. Both groups showed similar overall directional patterns for microsaccades. (**B**) Average direction of microsaccades in CB patients shown in polar coordinates and aligned to the center of mass of the blind field (90 degrees/up). (**C**) Average probability of microsaccades toward or away from the blind field in CB patients. Box boundaries represent the 25th and 75th percentiles, and individual data points reflect single-subject measurements. (**D**) Average ocular drift direction of CB patients (blue) and controls (red), plotted with respect to angle in real space. The scales in (**A**) and (**D**) are normalized probabilities, and the dashed lines in the polar plot represent 95% confidence intervals. (**E**) Average drift direction in CB patients aligned with the blind-field center of mass at 90 degrees. (**F**) Average probability of drift toward or away from the blind field in CB patients. Same conventions as in (**C**). n.s. denotes a lack of statistical significance; * denotes statistical significance with all descriptive statistics reported in the main text.

amplitude was larger toward the blind field, ocular drift exhibited a subtle but significant bias away from the blind field.

Fixational behavior during the acuity task

In the fixation task, participants were simply instructed to maintain fixation on a central target. This raises the question of whether the gaze offsets observed in CB patients under these relatively passive conditions would also be present when participants were engaged in a target identification task at fixation. To address this, we analyzed data from participants during an interleaved, four-alternative forced-choice number acuity task performed at fixation. Importantly, acuity thresholds were comparable between CB patients and controls under habitual correction (patients: 20/35, controls: 20/25; $t_{27} = 1.8$, $p = 0.07$, Cohen's $d = 0.6$) and under best correction using the Badal optometer setup (patients: 1.7 ± 1.0 MAR, controls: 1.2 ± 0.39 MAR; $t_{27} = 1.45$, $p = 0.15$, Cohen's $d = 0.5$; Supplementary Figure S4).

Just as during fixation trials, fixation precision in acuity trials, measured via BCEA, was similar between the two groups (patients: 0.1 ± 0.03 deg^2, controls: 0.09 ± 0.03 deg^2; $t_{27} = 0.87$, $p = 0.38$, Cohen's $d = 0.3$; Figure 8).

In contrast to the sustained fixation condition, no systematic differences in the magnitude of the gaze offset were observed between patients and controls during the acuity task: Patients no longer displayed a gaze offset toward their blind field, and gaze offset was now similar in the two groups (patients: 0.5′ ± 3′, controls: –0.1′ ± 2.7′; $t_{27} = 0.6$, $p = 0.5$, Cohen's $d = 0.2$; Figure 9). Thus, it appears that the small fixational offsets in CB patients occurred only during sustained fixation, not during a number identification/acuity task at fixation.

Just as in the sustained fixation task, microsaccade rate was comparable between CB patients and controls (patients: 0.8 ± 0.49 microsaccades/s; controls: 0.7 ± 0.4 microsaccades/s; two-tailed unpaired t-test: $t_{27} = 0.5$, $p = 0.61$, Cohen's $d = 0.18$), and there was no significant difference in the overall direction of microsaccades across groups (Figure 10A; 0–180 degrees vs. 180–360 degrees, unpaired t-test: $t_{26} =$

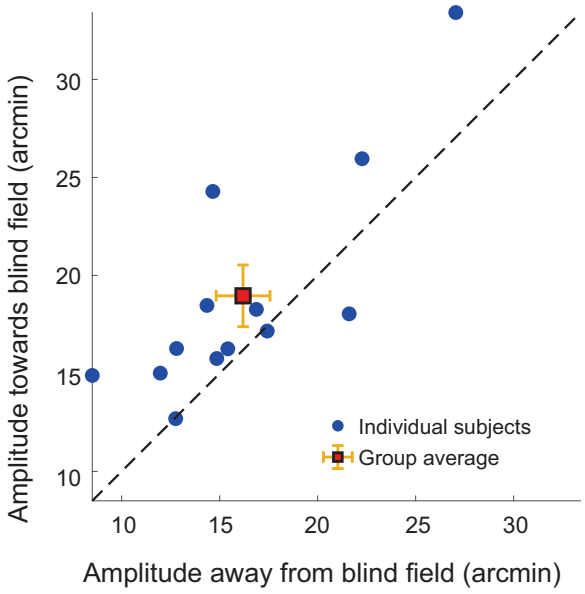

Figure 7. **Amplitude of microsaccades relative to blind field during early fixation (first 500 ms).** Patients made larger-amplitude microsaccades toward the blind field compared to away from it (difference: 2.7 ± 3.4 arcmin, $p = 0.01$, paired *t*-test).

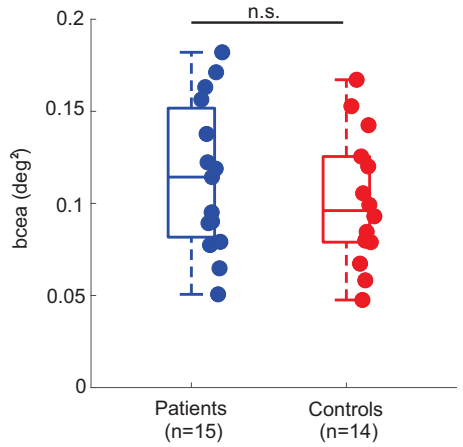

Figure 8. **Fixation stability during the acuity task.** BCEA in patients (mean = 0.1 ± 0.03 deg^2) and controls (0.09 ± 0.03 deg^2) showing no significant (n.s.) difference between the two groups (see main text for statistics). Box boundaries represent the 25th and 75th percentiles; individual data points reflect single-subject measurements.

-1.43, $p = 0.16$, Cohen's $d = -0.5$). Likewise, ocular drift characteristics did not differ significantly between patients and controls (Figure 10D; 0–180 degrees vs. 180–360 degrees, unpaired *t*-test: $t_{27} = -1.84$, $p = 0.07$, Cohen's $d = -0.6$). However, despite the absence of a measurable gaze offset toward the blind field during the acuity task, the underlying oculomotor behavior closely resembled that of the fixation-only condition: Microsaccades were unbiased (54% ± 24% toward the blind field vs. 45% ± 24% away from the blind field; $t_{13} = 0.6$, $p = 0.5$, Figure 10B, 10C), whereas ocular drift direction was biased away from the blind field (12% ± 4% toward vs. 17% ± 5% away; $t_{14} = -2.5$, $p = 0.02$, Figure 10E, 10F). In sum, microsaccade and drift behavior during the acuity task was largely comparable between CB patients and controls, and it mirrored patterns observed during sustained fixation.

Discussion

Despite the primary impact of stroke-induced CB on peripheral (rather than foveal) vision, our study has revealed the presence of a systematic change in fixation accuracy and the direction of ocular drifts in individuals with this condition. While patients and controls demonstrated comparable foveal visual acuity and fixational precision, patients exhibited a bias in gaze position on the order of ∼0.05 degrees of visual angle toward their blind field during fixation. Interestingly, this offset was not present during a high-acuity task performed at fixation. Additionally, in both task conditions, ocular drifts tended to move gaze away from the blind field. Microsaccades were evenly distributed toward and away from the blind field but were larger in amplitude when directed toward the blind field. Thus, our data highlight the far-reaching effects of peripheral deficits in unilateral CB on fixational eye movements.

Crucially, the bias reported here was unlikely to be an artifact of the eye-tracking calibration; whereas a simple 9-point calibration procedure would likely hide a systematic offset in gaze position, because it assumes that subjects are accurately fixating on the calibration markers, our dual-step manual calibration procedure (Poletti & Rucci, 2016; Santini et al., 2007) ensures that subjects are engaged in an active fixation task requiring them to align the system's estimate of gaze position with their perceived gaze position—something that can only be done accurately if subjects maintain fixation on the markers of the calibration grid. Furthermore, before every trial, subjects performed a recalibration procedure for the central point to ensure that accurate alignment of the perceived gaze position with the central fixation marker was maintained throughout the experiment. Finally, the presence of a gaze offset in a fixation task but not in the interleaved acuity task, and the fact that the bias was systematically in the direction of the blind field of patients, further confirmed that the observed bias was not the result of an eye-tracking artifact. These findings complement and refine previous reports of altered fixation behavior in hemianopic patients.

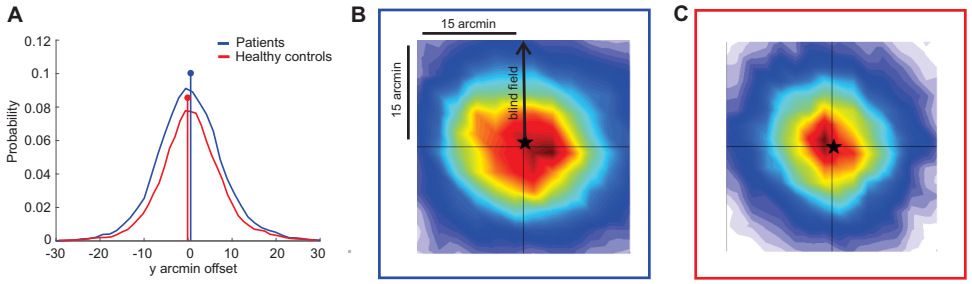

Figure 9. **Two-dimensional gaze distribution during the acuity task.** (**A**) Average gaze probability along the vertical (y) axis when gaze distributions (and visual deficits) are rotated to position the deficit's center of mass at 90 degrees vertical. In contrast with the fixation task, neither patients nor controls exhibited a significant gaze offset along the vertical (y) axis. (**B**) Two-dimensional gaze distributions across all patients, with gaze maps rotated such that the midline of the blind-field deficit faced upward (90 degrees). (**C**) Corresponding gaze distributions in healthy controls during the acuity task, shown in true (unrotated) visual space. Black stars (in **B, C**) indicate the average gaze offset from the center fixation (0, 0).

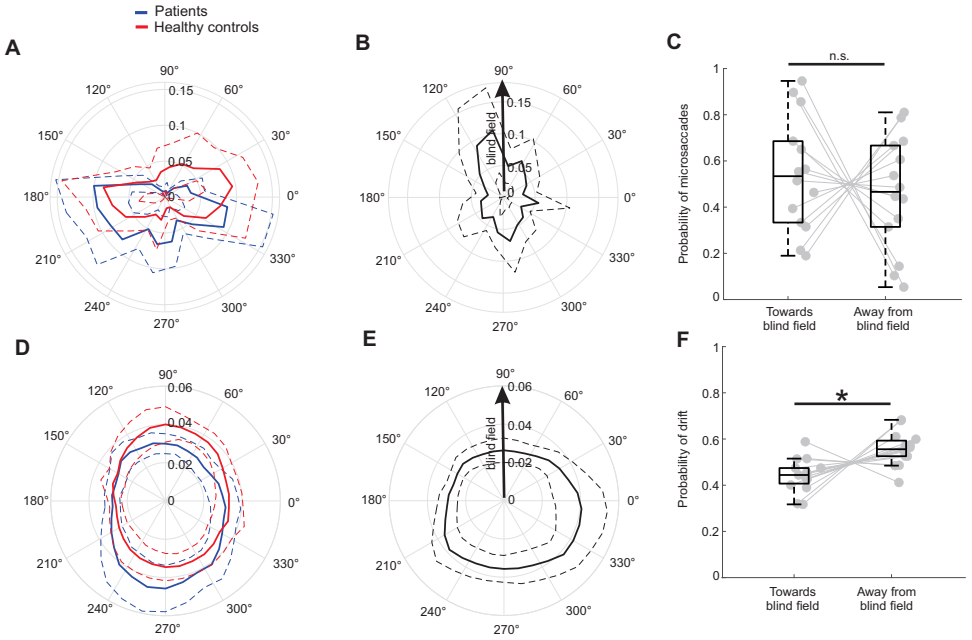

Figure 10. **Microsaccade and drift characteristics during the acuity task.** (**A**) Average microsaccade direction of CB patients (blue) and controls (red), plotted with respect to angle in real space. Both groups showed similar overall directional patterns for microsaccades. (**B**) Average direction of microsaccades in CB patients shown in polar coordinates and aligned to the center of mass of the blind field (90 degrees/up). (**C**) Average probability of microsaccades toward or away from the blind field in CB patients. Box boundaries represent the 25th and 75th percentiles, and individual data points reflect single-subject measurements. (**D**) Average ocular drift direction of CB patients (blue) and controls (red), plotted with respect to angle in real space. The scales in (**A**) and (**D**) are normalized probabilities, and the dashed lines in the polar plot represent 95% confidence intervals. (**E**) Average drift direction in CB patients aligned with the blind-field center of mass at 90 degrees. (**F**) Average probability of drift toward or away from the blind field in CB patients. Same conventions as in (**C**). n.s. denotes a lack of statistical significance; * denotes statistical significance with all descriptive statistics reported in the main text.

Our results differ from those reported by Gao and Sabel (2017), who used a commercial video-based eye tracker and found that microsaccades were biased toward the intact field in about half of their patients. Here, we show that microsaccades do not present a consistent bias either toward or away from the blind field, although microsaccades toward the blind field were slightly larger in amplitude. On the other hand, our findings are partly consistent with earlier work examining fixation behavior in hemianopic patients using a scanning laser ophthalmoscope to reconstruct eye movement trajectories and determine the precise

retinal location of the stimulus relative to the foveola (Trauzettel-Klosinski, 1997; Trauzettel-Klosinski & Reinhard, 1998). Trauzettel-Klosinski and colleagues reported that some—but not all—CB patients adopted an eccentric fixation locus in the seeing hemiretina during fixation tasks, even with preserved foveal function, thus shifting the field defect toward the blind hemifield. This shift was absent when subjects performed tasks requiring high spatial resolution. Although the gaze shifts reported were relatively large (1–2 degrees), our results parallel this finding at a much finer scale (<1 degree): During steady fixation, we found gaze to shift subtly toward the blind field, whereas in a high-acuity task requiring fine foveal resolution, fixation remained centered. Thus, using high-precision eye tracking, our study confirms and extends prior observations by showing that direction-specific asymmetries in gaze position during fixation are likely driven by systematic differences in the dynamics of ocular drift and microsaccades.

A bias of gaze position toward the blind field is reminiscent of what has been observed in this patient population for saccades, which are also biased toward the blind field (Iorizzo et al., 2011; Kerkhoff, 1999; Pambakian et al., 2000). The biased distribution of macro-saccades is an active strategy that allows patients to acquire information from an otherwise poorly utilized region of space (Kerkhoff, 1999). Given the tight link between saccades and attention (Tian, Yoshida, & Hafed, 2016; Zhao, Gersch, Schnitzer, Dosher, & Kowler, 2012), it is possible that this systematic behavior establishes an attentional pointer in the region of the blind field. The influence of such a pointer may be strongest when visual information is absent from the rest of the extrafoveal field (i.e., when there are no competing stimuli to capture attention and when fine foveal examination is not required for the task). This may explain our finding that microsaccade amplitude is slightly larger toward the blind field. An alternative but not mutually exclusive hypothesis comes from the primate animal model literature. Small gaze offsets during otherwise stable fixation have indeed been previously reported in studies inactivating the rostral part of one superior colliculus in macaques (Goffart, Hafed, & Krauzlis, 2012; Hafed, Goffart, & Krauzlis, 2008). These results were interpreted to support the "equilibrium hypothesis," which posits that fixation reflects an equilibrium of target-related activity balanced across the two superior colliculi. According to this hypothesis, localized suppression of activity in one colliculus would introduce a bias in the brain's internal estimate of the target's location (Krauzlis, Goffart, & Hafed, 2017). Since V1, which is damaged in our CB patients, provides direct input to its ipsilateral superior colliculus, V1 damage would represent a significant loss of drive to this subcortical center, likely altering the collicular "equilibrium" of activity across the two brain hemispheres. While it may be argued that the superior colliculus also receives input from other early visual areas (V2, V3, V4, MT) (Hafed, Hoffmann, Chen, & Bogadhi, 2023), this would not compensate for the loss of V1 input, as V1 damage significantly deafferents the same representation of the visual field in the extrastriate cortex. Thus, our patients' increased gaze offset toward their blind field during fixation of a central target could reflect a disrupted equilibrium between the two colliculi and/or disruption of the bilateral activity of the medio-posterior cerebellum, another region that may play an important role in the adaptive control of gaze accuracy (Guerrasio, Quinet, Büttner, & Goffart, 2010). All in all, from a broader perspective, a hypothesis stemming from the present results, which could prove valuable to test, is that the presence of a systematic gaze offset toward a perimetrically defined visual deficit is diagnostic of unilateral damage in visual centers downstream from the retina, rather than ocular damage per se.

Also of interest is that the abnormal fixational behavior in CB patients occurred despite central vision—including acuity—being normal. Thus, as a consequence of attentional biases toward the blind field, alteration of the normal activity balance between the two superior colliculi (Goffart et al., 2012), or a combination of both, a unilateral loss of peripheral vision due to cortical damage can influence the mechanisms controlling fixation stability. When not performing the acuity task, the mean fixation position in CB patients was systematically biased toward the blind field, and ocular drift showed a subtle bias away from it. This apparent dissociation suggests that while the overall fixation strategy favors directing gaze toward the region of vision loss—possibly to enhance perceptual coverage—slow drift movements may compensate, pulling gaze slightly back toward the seeing field. The net result is a stable fixation offset that reflects both strategic bias and local oculomotor dynamics.

Finally, we acknowledge that the magnitude of fixational offsets observed here (~3 arcmin or ~0.05 degrees on average) is likely too small to significantly impact visual performance. However, given the active development of different visual rehabilitation protocols for CB that rely on precise delivery of visual stimuli to regions of the blind or intact hemifields of vision (reviewed in Cavanaugh, Fahrenthold, & Huxlin, 2025; Saionz, Busza, & Huxlin, 2022; Saionz, Feldon, & Huxlin, 2021), the approach described here should be used in future studies to carefully measure fixational gaze patterns during such *peripheral* stimulus presentations. While the present results would predict that gaze offsets toward the blind field should be absent during peripheral task performance, empirical

confirmation is key to further guide and optimize the development of therapeutic interventions for this patient population.

Keywords: microsaccades, ocular drift, hemianopia, occipital stroke, V1, acuity

Acknowledgments

The authors thank Terrance Schaefer and Rachel Hollar for performing all Humphrey visual field tests analyzed presently and the participants for their invaluable contribution to this research.

Supported by the National Institutes of Health through grants R01 EY029788 (to MP), R01 EY027314 and R01 EY021209 (to KRH), Center Core Grant P30 EYE001319 and Training Grant T32 EY007125 to the Center for Visual Science, and an unrestricted grant from Research to Prevent Blindness (RPB) to the Flaum Eye Institute.

Commercial relationships: none.
Corresponding author: Krystel R. Huxlin.
Email: khuxlin@ur.rochester.edu.
Address: Department of Ophthalmology, University of Rochester, Rochester, NY 14627, USA.

*AMC and SK are equal first authors.
†KRH and MP are equal senior authors.

References

Ahissar, E., & Arieli, A. (2012). Seeing via miniature eye movements: A dynamic hypothesis for vision. *Frontiers in Computational Neuroscience, 6*, 89.

Anderson, A. G., Ratnam, K., Roorda, A., & Olshausen, B. A. (2020). High-acuity vision from retinal image motion. *Journal of Vision, 20*(7), 34, https://doi.org/10.1167/jov.20.7.34.

Atchison, D. A., Bradley, A., Thibos, L., & Smith, G. (1995). *Useful variations of the Badal optometer. Paper presented at the Vision Science and Its Applications*.

Barlow, H. B. (1952). Eye movements during fixation. *The Journal of Physiology, 116*(3), 290.

Bauer, C. M., Manley, C. E., Ravenscroft, J., Cabral, H., Dilks, D. D., & Bex, P. J. (2023). Deficits in face recognition and consequent quality-of-life factors in individuals with cerebral visual impairment. *Vision, 7*(1), 9.

Bowers, A. R., Keeney, K., & Peli, E. (2008). Community-based trial of a peripheral prism visual field expansion device for hemianopia. *Archives of Ophthalmology, 126*(5), 657–664.

Cavanaugh, M. R., Barbot, A., Carrasco, M., & Huxlin, K. R. (2019). Feature-based attention potentiates recovery of fine direction discrimination in cortically blind patients. *Neuropsychologia, 128*, 315–324.

Cavanaugh, M. R., Carrasco, M., & Huxlin, K. R. (2025). Exogenous spatial attention helps overcome spatial specificity of visual learning in the blind field after V1 damage. *Journal of Cognitive Enhancement, 9*(1), 21–37.

Cavanaugh, M. R., Fahrenthold, B. K., & Huxlin, K. R. (2025). What V1 damage can teach us about visual perception and learning. *Annual Review of Vision Science, 11*, 217–241.

Cavanaugh, M. R., Tadin, D., Carrasco, M., & Huxlin, K. R. (2022). Benefits of endogenous spatial attention during visual double-training in cortically-blinded fields. *Frontiers in Neuroscience, 16*, 771623.

Cherici, C., Kuang, X., Poletti, M., & Rucci, M. (2012). Precision of sustained fixation in trained and untrained observers. *Journal of Vision, 12*(6), 31, https://doi.org/10.1167/12.6.31.

Clark, A. M., Intoy, J., Rucci, M., & Poletti, M. (2022). Eye drift during fixation predicts visual acuity. *Proceedings of the National Academy of Sciences, 119*(49), e2200256119.

Dogra, N., Redmond, B. V., Lilley, S., Johnson, B. A., Lam, B. L., Tamhankar, M., . . . Cavanaugh, M. R. (2024). Vision-related quality of life after unilateral occipital stroke. *Brain and Behavior, 14*(7), e3582.

Gao, Y., & Sabel, B. A. (2017). Microsaccade dysfunction and adaptation in hemianopia after stroke. *Restorative Neurology and Neuroscience, 35*(4), 365–376.

Gilhotra, J. S., Mitchell, P., Healey, P. R., Cumming, R. G., & Currie, J. (2002). Homonymous visual field defects and stroke in an older population. *Stroke, 33*(10), 2417–2420.

Giudice, N. A. (2018). Navigating without vision: Principles of blind spatial cognition. InMontello, D. R. (Ed.), *Handbook of behavioral and cognitive geography* (pp. 260–288). Edward Elgar.

Goffart, L., Hafed, Z. M., & Krauzlis, R. J. (2012). Visual fixation as equilibrium: Evidence from superior colliculus inactivation. *Journal of Neuroscience, 32*(31), 10627–10636.

Guerrasio, L., Quinet, J., Büttner, U., & Goffart, L. (2010). Fastigial oculomotor region and the control of foveation during fixation. *Journal of Neurophysiology, 103*(4), 1988–2001.

Hafed, Z. M., Goffart, L., & Krauzlis, R. J. (2008). Superior colliculus inactivation causes stable offsets in eye position during tracking. *Journal of Neuroscience, 28*(32), 8124–8137.

Hafed, Z. M., Hoffmann, K.-P., Chen, C.-Y., & Bogadhi, A. R. (2023). Visual functions of the primate superior colliculus. *Annual Review of Vision Science, 9*(1), 361–383.

Horton, J. C., Economides, J. R., & Adams, D. L. (2021). The mechanism of macular sparing. *Annual Review of Vision Science, 7*(1), 155–179.

Intoy, J., & Rucci, M. (2020). Finely tuned eye movements enhance visual acuity. *Nature Communications, 11*(1), 795.

Iorizzo, D. B., Riley, M. E., Hayhoe, M., & Huxlin, K. R. (2011). Differential impact of partial cortical blindness on gaze strategies when sitting and walking—an immersive virtual reality study. *Vision Research, 51*(10), 1173–1184.

Jung, J.-H., & Peli, E. (2018). Field expansion for acquired monocular vision using a multiplexing prism. *Optometry and Vision Science, 95*(9), 814–828.

Kerkhoff, G. (1999). Restorative and compensatory therapy approaches in cerebral blindness: A review. *Restorative Neurology and Neuroscience, 15*(2–3), 255–271.

Ko, H.-k., Snodderly, D. M., & Poletti, M. (2016). Eye movements between saccades: Measuring ocular drift and tremor. *Vision Research, 122*, 93–104.

Krauzlis, R. J., Goffart, L., & Hafed, Z. M. (2017). Neuronal control of fixation and fixational eye movements. *Philosophical Transactions of the Royal Society B: Biological Sciences, 372*(1718), 20160205.

Kwon, S., Fahrenthold, B. K., Cavanaugh, M. R., Huxlin, K. R., & Mitchell, J. F. (2022). Perceptual restoration fails to recover unconscious processing for smooth eye movements after occipital stroke. *Elife, 11*, e67573.

Pambakian, A. L. M., Wooding, D., Patel, N., Morland, A., Kennard, C., & Mannan, S. (2000). Scanning the visual world: a study of patients with homonymous hemianopia. *Journal of Neurology, Neurosurgery & Psychiatry, 69*(6), 751–759.

Pelli, D. G., Waugh, S. J., Martelli, M., Crutch, S. J., Primativo, S., Yong, K. X., … Yiltiz, H. (2016). A clinical test for visual crowding. *F1000Research, 81*(5), 1–20.

Poletti, M., Listorti, C., & Rucci, M. (2013). Microscopic eye movements compensate for nonhomogeneous vision within the fovea. *Current Biology, 23*(17), 1691–1695.

Poletti, M., & Rucci, M. (2016). A compact field guide to the study of microsaccades: Challenges and functions. *Vision Research, 118*, 83–97.

Pollock, A., Hazelton, C., Rowe, F. J., Jonuscheit, S., Kernohan, A., Angilley, J., … Campbell, P. (2019). Interventions for visual field defects in people with stroke. *Cochrane Database of Systematic Reviews,* 5, CD008388.

Ratnam, K., Domdei, N., Harmening, W. M., & Roorda, A. (2017). Benefits of retinal image motion at the limits of spatial vision. *Journal of Vision, 17*(1), 30, https://doi.org/10.1167/17.1.30.

Riddoch, G. (1917). Dissociation of visual perceptions due to occipital injuries, with especial reference to appreciation of movement. *Brain, 40*(1), 15–57.

Roth, T., Sokolov, A., Messias, A., Roth, P., Weller, M., & Trauzettel-Klosinski, S. (2009). Comparing explorative saccade and flicker training in hemianopia: A randomized controlled study. *Neurology, 72*(4), 324–331.

Rowe, F. J., & VIS Writing Group. (2017). Vision in stroke cohort: Profile overview of visual impairment. *Brain and Behavior, 7*(11), e00771.

Rucci, M., & Poletti, M. (2015). Control and functions of fixational eye movements. *Annual Review of Vision Science, 1*(1), 499–518.

Rucci, M., & Victor, J. D. (2015). The unsteady eye: an information-processing stage, not a bug. *Trends in Neurosciences, 38*(4), 195–206.

Saionz, E. L., Busza, A., & Huxlin, K. R. (2022). Rehabilitation of visual perception in cortical blindness. *Handbook of Clinical Neurology, 184*, 357–373.

Saionz, E. L., Feldon, S. E., & Huxlin, K. R. (2021). Rehabilitation of cortically induced visual field loss. *Current Opinion in Neurology, 34*(1), 67–74.

Sand, K., Midelfart, A., Thomassen, L., Melms, A., Wilhelm, H., & Hoff, J. (2013). Visual impairment in stroke patients—a review. *Acta Neurologica Scandinavica, 127*, 52–56.

Santini, F., Redner, G., Iovin, R., & Rucci, M. (2007). EyeRIS: A general-purpose system for eye-movement-contingent display control. *Behavior Research Methods, 39*(3), 350–364.

Shelchkova, N., Tang, C., & Poletti, M. (2019). Task-driven visual exploration at the foveal scale. *Proceedings of the National Academy of Sciences, 116*(12), 5811–5818.

Steinman, R. M., Haddad, G. M., Skavenski, A. A., & Wyman, D. (1973). Miniature Eye Movement: The pattern of saccades made by man during maintained fixation may be a refined but useless motor habit. *Science, 181*(4102), 810–819.

Tian, X., Yoshida, M., & Hafed, Z. M. (2016). A microsaccadic account of attentional capture and inhibition of return in Posner cueing. *Frontiers in Systems Neuroscience, 10*, 23.

Trauzettel-Klosinski, S. (1997). Eccentric fixation with hemianopic field defects: A valuable strategy to improve reading ability and an indication of cortical plasticity. *Neuro-ophthalmology, 18*(3), 117–131.

Trauzettel-Klosinski, S., & Reinhard, J. (1998). The vertical field border in hemianopia and its significance for fixation and reading. *Investigative Ophthalmology & Visual Science, 39*(11), 2177–2186.

Weiskrantz, L. (1996). Blindsight revisited. *Current Opinion in Neurobiology, 6*(2), 215–220.

Weiskrantz, L. (2009). Is blindsight just degraded normal vision? *Experimental Brain Research, 192*, 413–416.

Weiskrantz, L., Warrington, E. K., Sanders, M., & Marshall, J. (1974). Visual capacity in the hemianopic field following a restricted occipital ablation. *Brain, 97*(1), 709–728.

Wichmann, F. A., & Hill, N. J. (2001). The psychometric function: I. Fitting, sampling, and goodness of fit. *Perception & Psychophysics, 63*(8), 1293–1313.

Witten, J. L., Lukyanova, V., & Harmening, W. M. (2024). Sub-cone visual resolution by active, adaptive sampling in the human foveola. *Elife, 13*, RP98648.

Wu, R.-J., Clark, A. M., Cox, M. A., Intoy, J., Jolly, P. C., Zhao, Z., … Rucci, M. (2023). High-resolution eye-tracking via digital imaging of Purkinje reflections. *Journal of Vision, 23*(5), 4, https://doi.org/10.1167/jov.23.5.4.

Zhao, M., Gersch, T. M., Schnitzer, B. S., Dosher, B. A., & Kowler, E. (2012). Eye movements and attention: The role of pre-saccadic shifts of attention in perception, memory and the control of saccades. *Vision Research, 74*, 40–60.

Zihl, J., Kentridge, R., Pargent, F., & Heywood, C. (2021). Aging and the rehabilitation of homonymous hemianopia: The efficacy of compensatory eye-movement training techniques and a five-year follow up. *Aging Brain, 1*, 100012.